

Commensurate-incommensurate solid transition in the ^4He monolayer on γ -graphyne

Jeonghwan Ahn, Hoonkyung Lee, and Yongkyung Kwon*

Division of Quantum Phases and Devices, School of Physics, Konkuk University, Seoul 143-701, Korea

(Dated: March 1, 2022)

Path-integral Monte Carlo calculations have been performed to study the ^4He adsorption on γ -graphyne, a planar network of benzene rings connected by acetylene bonds. Assuming the ^4He -substrate interaction described by a pairwise sum of empirical ^4He -carbon interatomic potentials, we find that unlike α -graphyne, a single sheet of γ -graphyne is not permeable to ^4He atoms in spite of its large surface area. One-dimensional density distributions computed as a function of the distance from the graphyne surface reveal a layer-by-layer growth of ^4He atoms. A partially-filled ^4He monolayer is found to exhibit different commensurate solid structures depending on the helium coverage; it shows a $\text{C}_{2/3}$ commensurate structure at an areal density of 0.0491 \AA^{-2} , a $\text{C}_{3/3}$ structure at 0.0736 \AA^{-2} , and a $\text{C}_{4/3}$ structure at 0.0982 \AA^{-2} . While the promotion to the second layer starts beyond the $\text{C}_{4/3}$ helium coverage, the first ^4He layer is found to form an incommensurate triangular solid when compressed with the development of the second layer.

PACS numbers: 67.25.bd, 67.25.bh, 67.80.B-, 75.10.-b

For the past few decades, a system of ^4He atoms adsorbed on a substrate has been intensively studied to investigate physical properties of low-dimensional quantum fluids. Carbon allotropes have often been chosen as substrates for this purpose because they provide strong enough interactions for ^4He adsorbates to show multiple distinct layered structures [1]. As a result of the interplay between ^4He - ^4He and ^4He -substrate interaction, these helium adlayers are known to exhibit rich phase diagrams including various commensurate and incommensurate solids. On the surface of graphite, a monolayer of ^4He atoms is crystallized to a $\text{C}_{1/3}$ commensurate solid at an areal density of 0.0636 \AA^{-2} and goes through various domain structures before freezing into an incommensurate triangular solid as the helium coverage increases [2, 3]. Similar quantum phase transitions were predicted for the ^4He monolayer on a single graphene sheet [4–6]. While no superfluidity has been observed in the first ^4He layer, the second layer on graphite does show finite superfluid response at intermediate helium coverages as first revealed by torsional oscillator measurements of Crowell and Reppy [3]. Whether this second-layer superfluid phenomenon is related to two-dimensional superfluidity is still an ongoing issue pursued heavily by some experimentalists.

The ^4He adsorption on the surface of a carbon allotrope other than graphite or graphene has recently been investigated. While ^4He atoms adsorbed on the interstitials or the grooves of carbon nanotube bundles showed characteristics of one-dimensional quantum fluid [7, 8], a series of theoretical calculations predicted well-distinct layered structures for ^4He atoms adsorbed on the outer surfaces of fullerene molecules with each near-spherical helium layer exhibiting various quantum states depending on the number of ^4He adatoms [9–12]. More recently, graphynes, sp - sp^2 hybridized two-dimensional networks of carbon atoms [13–15], have attracted much interest

because of their intriguing electronic features such as both symmetric and asymmetric Dirac cones [16, 17] and high carrier mobility [18]. Furthermore, they have much larger surface area than graphene, which has prompted intensive investigation of their possible applications as high-capacity hydrogen storage [19, 20] and Li-ion battery anode materials [21]. Using the path-integral Monte Carlo (PIMC) method, one of us recently studied the ^4He adsorption on α -graphyne [22], a honeycomb structure of both sp^2 -bonded carbon atoms and sp -bonded ones. Due to the presence of much larger hexagons than those of graphene, in-plane adsorption of ^4He atoms was observed on α -graphyne with a single ^4He atom being embedded to the center of each hexagon. The first layer of ^4He atoms adsorbed on the ^4He -embedded α -graphyne was found to undergo a Mott-insulator to commensurate-solid transition which was interpreted as a transition from a spin liquid of frustrated antiferromagnets to a ferromagnetic phase with the introduction of Ising pseudospins based on the sublattice symmetry of the honeycomb structure [22].

Here we have performed the PIMC simulations to study the ^4He adsorption on γ -graphyne, the most stable structure among graphynes [23]. With the increasing number of ^4He adatoms, multiple distinct helium layers are observed on γ -graphyne. Because of larger hexagons of graphyne, these ^4He adsorbates show a richer phase diagram than the corresponding ones on graphite or graphene. Unlike α -graphyne, however, even a single sheet of γ -graphyne is found to be impermeable to ^4He atoms. It is found that the ^4He monolayer exhibits various commensurate solid structures at different areal densities before crystallizing into an incommensurate triangular solid at its completion.

In this study, a single γ -graphyne sheet is fixed at $z = 0$ and the helium-graphyne interaction is described by a sum of pair potentials between the carbon atoms and a ^4He atom. For the ^4He -C interatomic potential, we use

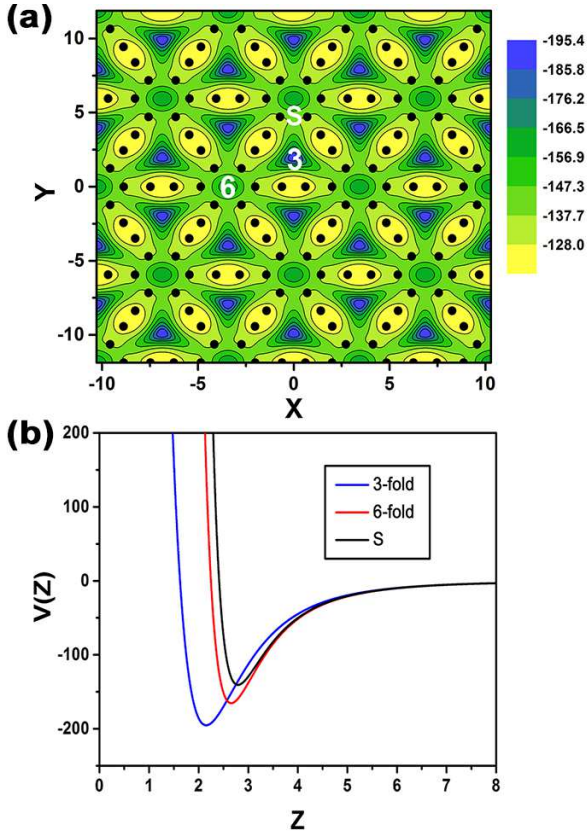


FIG. 1: (Color online) (a) A contour plot of the minimum ${}^4\text{He}$ -graphyne potential, $V_{\min}(x, y)$, above each point (x, y) on γ -graphyne and (b) the ${}^4\text{He}$ -graphyne potential as a function of the distance z from the graphyne surface along different symmetry directions. The black dots in (a) represent the positions of carbon atoms on the γ -graphyne surface. In (b), the blue, the red, and the black line correspond to the 3-fold symmetry direction, the 6-fold direction, and the direction of a saddle point (see white numbers and alphabet S in (a)), respectively. The length unit is \AA and the potential energies are in units of Kelvin.

an isotropic 6-12 Lennard-Jones potential proposed by Carlos and Cole [24] to fit helium scattering data from graphite surfaces. While Fig. 1(a) shows a contour plot of the minimum potential energy, $V_{\min}(x, y)$, above each point (x, y) on the graphyne surface, Fig. 1(b) presents our ${}^4\text{He}$ -graphyne potential as a function of the distance z from graphyne along three different symmetry directions perpendicular to the graphyne surface. As seen in Fig. 1(a), there are three adsorption sites per graphyne unit cell, two global minima of the ${}^4\text{He}$ -graphyne potential located at the centers of big irregular hexagons and one local minimum located at the center of a small regular hexagon (or a benzene ring). A bigger hexagon, which has much larger area than a smaller one, is expected to accommodate more than one ${}^4\text{He}$ atom. Figure 1(b) shows that the global minima in the three-fold symmetry directions are located closer to the graphyne

surface by $\sim 0.5 \text{ \AA}$ than the local minima in the six-fold symmetry directions and the potential energy difference between them is as large as $\sim 30 \text{ K}$. From this we conjecture that the ${}^4\text{He}$ adatoms predominantly occupy the global minimum sites at low helium coverages, rather than the local minima. We here note that there is strong repulsive potential barrier for ${}^4\text{He}$ atoms as they approach the graphyne surface, *i.e.*, $z \rightarrow 0$, suggesting that ${}^4\text{He}$ atoms cannot penetrate through a γ -graphyne sheet from one side to the other.

This approach of modeling ${}^4\text{He}$ -substrate potential with a pairwise sum of empirical interatomic potentials has been widely used to study the ${}^4\text{He}$ adsorptions on various carbon-based substrates, including α -graphyne [22]. For the ${}^4\text{He}$ - ${}^4\text{He}$ interaction, we use a well-known Aziz potential [25]. Since the exact form of thermal many-body density matrix is not known at a low temperature T , one can resort to the path-integral representation where the low-temperature density matrix is expressed by a convolution of M high-temperature density matrices with an imaginary time step $\tau = 1/(Mk_B T)$. Both ${}^4\text{He}$ - ${}^4\text{He}$ and ${}^4\text{He}$ -C pair potentials are used to derive the exact two-body density matrices at the high temperature MT [26, 27], which was found to provide accurate description of the ${}^4\text{He}$ -graphyne interaction as well as the ${}^4\text{He}$ - ${}^4\text{He}$ interaction with an imaginary time step of $(\tau k_B)^{-1} = 40 \text{ K}$. We employ the multilevel Metropolis algorithm described in Ref. [26] to sample the imaginary time paths as well as the permutations among ${}^4\text{He}$ atoms. To minimize finite size effects, periodic boundary conditions are applied to a fixed 3×2 rectangular simulation cell with dimensions of $20.58 \times 23.76 \text{ \AA}^2$. All PIMC simulations presented here started from random initial configurations of ${}^4\text{He}$ atoms.

Here we consider the ${}^4\text{He}$ adsorption only on one side of the graphyne sheet, *i.e.*, $z > 0$. Figure 2 presents one dimensional ${}^4\text{He}$ density distributions as a function of distance z from the graphyne surface for different numbers of ${}^4\text{He}$ adatoms N per 3×2 rectangular simulation cell. These density distributions confirm the above assertion that ${}^4\text{He}$ atoms cannot penetrate to the other side of $z < 0$ through a single graphyne sheet because of the presence of the strong repulsive potential barrier. As more ${}^4\text{He}$ atoms are adsorbed, one can see the development of layered structures as evidenced by well-distinct density peaks in Fig. 2. The first sharp peak is located at $z \sim 2.7 \text{ \AA}$ and the second peak at $z \sim 5.8 \text{ \AA}$, similar to the case of ${}^4\text{He}$ on graphene [5]. We observe the emergence of the ${}^4\text{He}$ second layer when the number of ${}^4\text{He}$ adatoms per 3×2 simulation cell increases beyond $N = 48$ (an areal density of 0.0982 \AA^{-2}). With further development of the second helium layer, more ${}^4\text{He}$ atoms are found to be squeezed into the first layer. From this we conjecture that the completed first layer would be a compressible incommensurate solid like the corresponding layer on graphene [5] or graphite [2, 28]. It is found

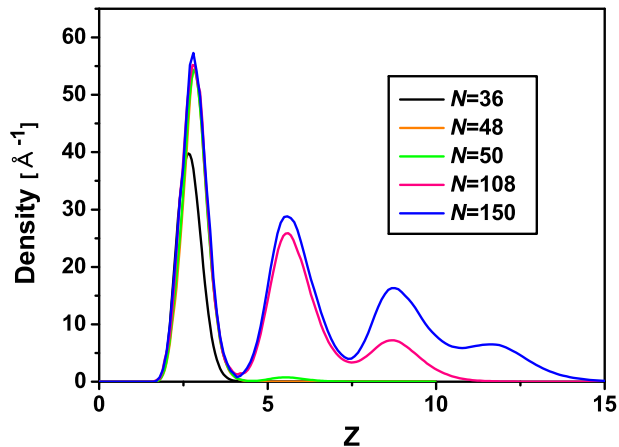


FIG. 2: (Color online) One-dimensional density of ^4He atoms adsorbed on a single γ -graphyne sheet as a function of the distance z (in \AA) from the graphyne surface. Here N represents the number of ^4He adatoms per 3×2 rectangular simulation cell with dimensions of $20.58 \times 23.76 \text{ \AA}^2$ and the computations were done at a temperature of 0.5 K.

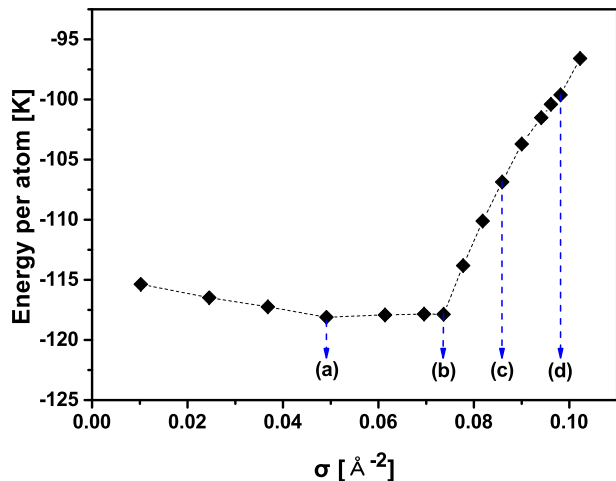


FIG. 3: (Color online) Energy per ^4He atom of the first ^4He layer on γ -graphyne as a function of the helium coverage. The alphabets (a), (b), (c), and (d) correspond to the areal densities of 0.0491, 0.0736, 0.0859, and 0.0982 \AA^{-2} , respectively, for which two-dimensional ^4He density plots are shown in Fig. 4. The energies were computed at a temperature of 0.5 K.

that the first layer is completed at an areal density of $\sim 0.115 \text{ \AA}^{-2}$ while the corresponding value on graphene was predicted to be $\sim 0.12 \text{ \AA}^{-2}$ [5]. This small (about 4 %) difference suggests that the ^4He -graphyne potential is more attractive than the ^4He -graphene potential and graphyne may accommodate more ^4He atoms in its immediate vicinity than graphene.

Now we discuss the energetics of the ^4He -graphyne system, which provides some insight into the growth of the ^4He adlayers on γ -graphyne and their different quantum phases. Figure 3 shows the energy per ^4He atom

as a function of an areal density σ . At low densities of $\sigma < 0.0736 \text{ \AA}^{-2}$, the energy per ^4He atom changes very little, indicating that each ^4He atom occupies one of the adsorption sites, *i.e.*, the ^4He -graphyne potential minima. It is found that the energy per atom has the lowest value at $\sigma = 0.0491 \text{ \AA}^{-2}$ which corresponds to two ^4He atoms per the graphyne unit cell. Noting that there are two global minima of the ^4He -graphyne potential per the unit cell (see Fig. 1(a)), we conjecture that in the lowest energy state at $\sigma = 0.0491 \text{ \AA}^{-2}$ each global minimum site is occupied by a single ^4He atom. After filling all global minima, additional ^4He atoms are expected to occupy the local minima located above the centers of the small hexagons, which is consistent with slight increase in the energy per atom for $0.0491 \text{ \AA}^{-2} < \sigma < 0.0736 \text{ \AA}^{-2}$. Since the distances between the adsorption sites on the graphyne surface are long enough ($\sim 4 \text{ \AA}$), the ^4He - ^4He interaction is understood to have minimal effects while ^4He atoms are filling these adsorption sites. Each adsorption site, whether it is a global minimum or a local minimum, is occupied by a single ^4He atom at an areal density of $\sigma = 0.0736 \text{ \AA}^{-2}$, three ^4He atoms per the graphyne unit cell, beyond which one can observe a sudden increase in the energy per atom in Fig. 3. The continuous increase of the energy per atom for $\sigma > 0.0736 \text{ \AA}^{-2}$ suggests that the ^4He - ^4He interaction as well as the ^4He -substrate interaction plays a critical role in determining quantum states of the ^4He monolayer at high helium coverages. One can observe a significant jump in the energy per atom at an areal density of $\sigma = 0.0982 \text{ \AA}^{-2}$, which reflects the start of the second-layer promotion concluded in the analysis of the one-dimensional density distributions of Fig. 2.

For further analysis of different phases of the ^4He monolayer, we computed two-dimensional density distributions of ^4He adatoms on γ -graphyne at various areal densities. In all four density plots presented in Fig. 4, a distinct density peak represents the occupancy of a single first-layer ^4He atom. At an areal density of 0.0491 \AA^{-2} , which corresponds to the lowest energy state, each of the irregular hexagons is seen in Fig. 4(a) to accommodate one ^4He atom at its center, confirming our conjecture made from the energetic analysis. These ^4He atoms form a honeycomb structure with the same primitive vectors as those of the underlying graphyne triangular lattice, which is therefore a 1×1 registered phase in the Wood's notation. It is also a $C_{2/3}$ commensurate solid with two out of every three adsorption sites being occupied by ^4He atoms. The lowest-energy state for the ^4He monolayer on graphene is a $C_{1/3}$ commensurate solid [4]. We note that the $C_{2/3}$ commensurate solid on graphyne is realized at an areal density significantly lower than the $C_{1/3}$ commensurate helium coverage of 0.0636 \AA^{-2} on graphene. Furthermore, vacancies created in this $C_{2/3}$ solid on graphyne are found to be immobile and very weakly, if ever, interacting with each other, which could be understood

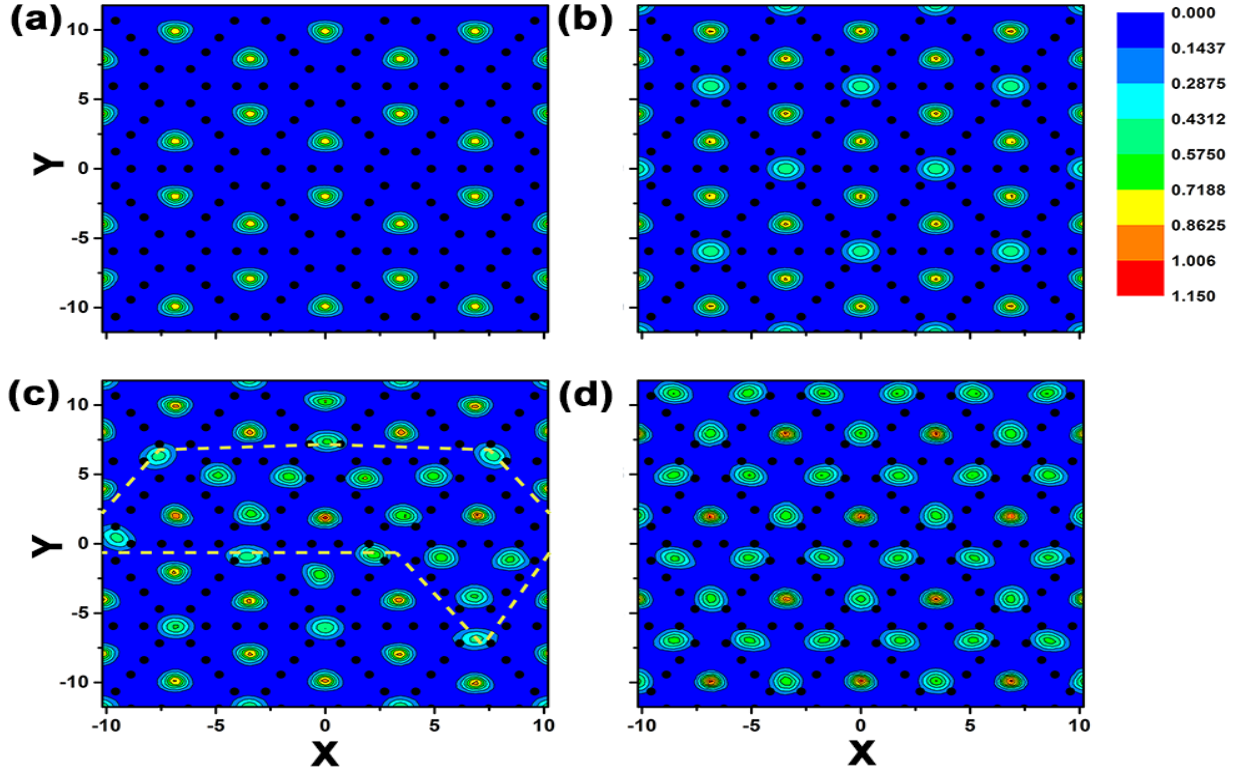


FIG. 4: (Color online) Two-dimensional density distributions of the first-layer ^4He atoms adsorbed on a single γ -graphyne sheet at areal densities of (a) 0.0491, (b) 0.0736, (c) 0.0859, and (d) 0.0982 \AA^{-2} . The black dots represent the positions of the carbon atoms of graphyne. The length unit is \AA and all contour plots are in the same color scale denoted by the color table in the upper right hand corner. The yellow dotted lines in (c) separate two different domains from each other. The PIMC calculations were done at a temperature of 0.5 K.

by high potential barrier and long distances between the neighboring adsorption sites.

As conjectured above, the local minima located at the centers of the small regular hexagons accommodate additional ^4He atoms beyond the $\text{C}_{2/3}$ commensurate coverage. Figure 4(b) shows another commensurate structure at an areal density of $\sigma = 0.0736 \text{ \AA}^{-2}$, where each of the adsorption sites, both global minima and local minima, is occupied by a single ^4He atom. In this $\text{C}_{3/3}$ commensurate structure, the ^4He adatoms form a triangular solid structure registered by $\frac{1}{\sqrt{3}} \times \frac{1}{\sqrt{3}}$ to the graphyne triangular lattice. With further increase of the helium coverage beyond the $\text{C}_{3/3}$ solid, where the energy per ^4He atom increases monotonically as shown in Fig. 3, the ^4He monolayer enters a regime of various domain structures. At higher ^4He coverages, the ^4He - ^4He interaction as well as the ^4He -substrate interaction is expected to affect the structure of the ^4He monolayer. At an areal density of 0.0859 \AA^{-2} , one can observe two different domains separated by the yellow dotted lines in Fig. 4(c); one domain involves some irregular hexagons accommodating three ^4He atoms while the other consists of the ^4He atoms in the $\text{C}_{3/3}$ commensurate order. Another homogeneous phase of the ^4He monolayer is ob-

served at an areal density of 0.0982 \AA^{-2} , where all ^4He atoms are accommodated by irregular hexagons and no small hexagon includes a ^4He atom. In this phase, some irregular hexagons accommodate three ^4He atoms and the neighboring ones include only one ^4He atom. With an alternating order of the three-atom and the single-atom irregular hexagons, the ^4He atoms constitute another perfect triangular solid whose primitive vectors are one half of those of the underlying graphyne structure. This $\frac{1}{2} \times \frac{1}{2}$ registered phase is a $\text{C}_{4/3}$ commensurate solid with 4 ^4He atoms being accommodated by a graphyne unit cell. We note that Li atoms attached to γ -graphyne could constitute an in-plane structure similar to this $\text{C}_{4/3}$ solid as reported in Ref. [21]. As discussed above, the ^4He adatoms start to get promoted to the second layer beyond the $\text{C}_{4/3}$ commensurate coverage of 0.0982 \AA^{-2} . With further development of the second ^4He layer, more ^4He atoms are found to be squeezed into the first layer. The fully-compressed first layer shows an incommensurate triangular lattice structure like the corresponding layer on graphite.

Our PIMC calculations have showed multiple distinct ^4He layers on a single sheet of γ -graphyne which is not permeable to ^4He atoms unlike α -graphyne. The ^4He

monolayer on γ -graphyne is found to exhibit various commensurate structures depending on the helium coverage, including the 1×1 , the $\frac{1}{\sqrt{3}} \times \frac{1}{\sqrt{3}}$, and the $\frac{1}{2} \times \frac{1}{2}$ registered phases. While some theoretical calculations predicted that zero-point vacancies would not be thermodynamically stable in bulk solid ^4He [29–31], a substrate potential could stabilize the vacancy formation in a commensurate ^4He solid on a substrate. Therefore the existence of a stable commensurate structure is understood to be critical in realizing the vacancy-based supersolidity proposed originally by Andreev and Lifshitz [32]. One of several commensurate structures we found in the ^4He monolayer on γ -graphyne could manifest the superfluid response induced by vacancies, which is now under our investigation.

This work was supported by the Basic Science Research Program (2012R1A1A2006887) through the National Research Foundation of Korea funded by the Ministry of Education, Science and Technology. We also acknowledge the support from the Supercomputing Center/Korea Institute of Science and Technology Information with supercomputing resources including technical support (KSC-2013-C3-033).

* Electronic address: ykwon@konkuk.ac.kr

- [1] G. Zimmerli, G. Mistura, and M. H. W. Chan, Phys. Rev. Lett. **68**, 60 (1992).
- [2] D. S. Greywall, Phys. Rev. B **47**, 309 (1993).
- [3] P. A. Crowell and J. D. Reppy, Phys. Rev. B **53**, 2701 (1996).
- [4] M. C. Gordillo and J. Boronat, Phys. Rev. Lett. **102**, 085303 (2009).
- [5] Y. Kwon and D. M. Ceperley, Phys. Rev. B **85**, 224501 (2012).
- [6] J. Happacher, P. Corboz, M. Boninsegni, and L. Pollet, Phys. Rev. B **87**, 094514 (2013).
- [7] M. W. Cole, V. H. Crespi, G. Stan, C. Ebner, J. M. Hartman, S. Moroni, and M. Boninsegni, Phys. Rev. Lett. **84**, 3883 (2000).
- [8] M. C. Gordillo, Phys. Rev. Lett. **101**, 046102 (2008).
- [9] Y. Kwon and H. Shin, Phys. Rev. B **82**, 172506 (2010).
- [10] H. Shin and Y. Kwon, J. Chem. Phys. **136**, 064514 (2012).
- [11] H. Shin and Y. Kwon, J. Chem. Phys. **138**, 064307 (2013).
- [12] S. Park and Y. Kwon, Phys. Rev. E **89**, 042118 (2014).
- [13] R. H. Baughman, H. Eckhardt, and M. Kertesz, J. Chem. Phys. **87**, 6687 (1987).
- [14] V. R. Coluci, S. F. Braga, S. B. Legoas, D. S. Galvão, and R. H. Baughman, Phys. Rev. B **68**, 035430 (2003).
- [15] V. R. Coluci, S. F. Braga, S. B. Legoas, D. S. Galvão, and R. H. Baughman, Nanotechnology **15**, S142 (2004).
- [16] D. Malko, C. Neiss, F. Viñes, and A. Görling, Phys. Rev. Lett. **108**, 086804 (2012).
- [17] B. G. Kim and H. J. Choi, Phys. Rev. B **86**, 115435 (2012).
- [18] J. Chen, J. Xi, D. Wang, and Z. Shuai, J. Phys. Chem. Lett. **4**, 1443 (2013).
- [19] H. Hwang, Y. Kwon, and H. Lee, J. Phys. Chem. C **116**, 20220 (2012).
- [20] J. Koo, H. Hwang, B. Huang, H. Lee, H. Lee, M. Park, Y. Kwon, S.-H. Wei, and H. Lee, J. Phys. Chem. C **117**, 11960 (2013).
- [21] H. Hwang, J. Koo, M. Park, N. Park, Y. Kwon, and H. Lee, J. Phys. Chem. C **117**, 6919 (2013).
- [22] Y. Kwon, H. Shin, and H. Lee, Phys. Rev. B **88**, 201403(R) (2013).
- [23] H. Shin, S. Kang, J. Koo, H. Lee, J. Kim, and Y. Kwon, J. Chem. Phys. **140**, 114702 (2014).
- [24] W. E. Carlos and M. W. Cole, Surf. Sci. **91**, 339 (1980).
- [25] R. A. Aziz, M. J. Slaman, A. Koide, A. R. Allnatt, and W. J. Meath, Mol. Phys. **77**, 321 (1992).
- [26] D. M. Ceperley, Rev. Mod. Phys. **67**, 279 (1995).
- [27] R. E. Zillich, F. Paesani, Y. Kwon, and K. B. Whaley, J. Chem. Phys. **123**, 114301 (2005).
- [28] P. Corboz, M. Boninsegni, L. Pollet, and M. Troyer, Phys. Rev. B **78**, 245414 (2008).
- [29] D. M. Ceperley and B. Bernu, Phys. Rev. Lett. **93**, 155303 (2004).
- [30] B. K. Clark and D. M. Ceperley, Phys. Rev. Lett. **96**, 105302 (2006).
- [31] M. Boninsegni, A. B. Kuklov, L. Pollet, N. V. Prokof'ev, B. V. Svistunov, and M. Troyer, Phys. Rev. Lett. **97**, 080401 (2006).
- [32] A. F. Andreev and I. M. Lifshitz, Sov. Phys. JETP **29**, 1107 (1969).